

# Psychophysical recovery from single-pulse forward masking in electric hearing

David A. Nelson<sup>a)</sup> and Gail S. Donaldson

*Clinical Psychoacoustics Laboratory, University of Minnesota, MMC 396, 420 Delaware St. S.E., Minneapolis, Minnesota 55455*

(Received 10 October 2000; revised 9 March 2001; accepted 20 March 2001)

Psychophysical single-pulse forward-masking (SPFM) recovery functions were measured for three electrodes in each of eight subjects with the nucleus mini-22 cochlear implant. Masker and probe stimuli were single 200- $\mu$ s/phase biphasic current pulses. Recovery functions were measured at several masker levels spanning the electric dynamic range of electrodes chosen from the apical, middle, and basal regions of each subject's electrode array. Recovery functions were described by an exponential process in which threshold shift (in  $\mu$ A) decreased exponentially with increasing time delay between the masker and probe pulses. Two recovery processes were observed: An initial, rapid-recovery process with an average time constant of 5.5 ms was complete by about 10 ms. A second, slow-recovery process involved less masking than the rapid-recovery process but encompassed much longer time delays, sometimes as long as several hundred milliseconds. Growth-of-masking slopes for the rapid process depended upon time delay, as expected in an exponential recovery process. Unity slopes were observed at a time delay of 0 ms, whereas progressively shallower slopes were observed at time delays of 2 ms and 5 ms. Many recovery functions demonstrated nonmonotonicities or "facilitation" at very short masker-probe delays (1–2 ms). Such nonmonotonicities were usually most pronounced at low masker levels. Time constants for the rapid-recovery process did not vary systematically with masker level or with electrode location along the implanted array. Most subjects demonstrated rapid-recovery time constants less than 7 ms; however, the subject with the longest duration of deafness prior to implantation exhibited clearly prolonged time constants (9–24 ms). Time constants obtained on basal electrodes were inversely related to word recognition scores. © 2001 Acoustical Society of America.  
[DOI: 10.1121/1.1371762]

PACS numbers: 43.66.Dc, 43.66.Mk, 43.66.Ts, 43.64.Me [SPB]

## I. INTRODUCTION

This paper describes psychophysical forward-masking recovery functions obtained in human cochlear implant listeners using a specific stimulus paradigm in which both masker and probe stimuli are single, biphasic current pulses. We refer to this paradigm as "single-pulse forward masking" (SPFM). SPFM recovery functions are of interest because they are thought to reflect the refractory characteristics of underlying peripheral auditory nerve fibers (ANFs). Because neural degeneration is likely to alter ANF refractory properties, SPFM recovery functions may provide an indication of peripheral auditory neural status in cochlear implant patients and may help to explain differences in subjects' performance on psychophysical and speech recognition tasks. It is important to distinguish SPFM from pulse-train forward masking (PTFM), which uses longer duration probe and masker signals, since the two paradigms yield recovery functions with quite different characteristics (Donaldson and Nelson, 1999). Although differences between SPFM and PTFM are not well understood, it is likely that SPFM provides a more direct measure of short-term recovery processes than PTFM (Donaldson and Nelson, 1999) and that SPFM is less

affected than PTFM by central auditory phenomena such as temporal pattern recognition (Blamey and Dooley, 1993).

Physiological SPFM recovery functions have been reported in animals with implanted electrode arrays (Stypulkowski and van den Honert, 1984; Miller *et al.*, 1993; Zhou *et al.*, 1995) and in human cochlear implant listeners (Brown *et al.*, 1990; Abbas and Brown, 1991; Brown *et al.*, 1996; Hong *et al.*, 1998). Such functions are obtained by presenting two identical current pulses in close succession and measuring the amplitude of the neural response to the second pulse as a function of inter-pulse time delay. In general, reported functions follow an exponential time course of recovery with time constants less than 5 ms. Animal studies indicate that recovery time constants vary with spike-initiation site and with the morphological characteristics of fibers in deafened ears (Stypulkowski and van den Honert, 1984; Miller *et al.*, 1993; Zhou *et al.*, 1995). An intriguing aspect of some physiologic SPFM functions is the existence of level-dependent nonmonotonicities at very short time delays (<2 ms) (Stypulkowski and van den Honert, 1984; Miller *et al.*, 1993).

Brown *et al.* (1996) obtained both physiological and psychophysical SPFM functions in a group of human cochlear implant listeners. Psychophysical and physiological functions had similar recovery characteristics in many subjects, suggesting that psychophysical SPFM measures are

<sup>a)</sup> Author to whom correspondence should be addressed. Electronic mail: dan@tc.umn.edu

TABLE I. Subjects. Subject identifying code, gender, age when tested for the present study, etiology of deafness (implanted ear), duration of bilateral severe-to-profound hearing loss prior to implantation, depth of electrode array insertion (mm from the round window, with 25 mm representing complete insertion), duration of implant use prior to the study, and percent-correct score on the NU-6 monosyllabic word test in quiet. NU-6 scores were obtained at a presentation level of 65 dB SPL with subjects using their own speech processor programmed in the MPEAK (subject EJQ) or SPEAK (all other subjects) speech processing strategy.

Subject code	M/F	Age	Etiology of deafness	Dur. (years)	Depth (mm)	CI use (years)	NU-6 (% C)
AGF	m	79	Noise exposure; progressive SNHL	25	20	8	6
AMB	m	56	Familial progressive SNHL	1	25	7	68
CJP	m	31	Maternal rubella; progressive SNHL	<1	23	2	70
DAW	f	59	Otosclerosis	10	25	1	40
EJQ	f	54	Mumps; progressive SNHL	9	22	10	0
GPB	m	59	Meningitis	<1	25	2	28
JPB	m	61	Progressive SNHL	4	24	9	70
RFM	m	66	Meniere's disease	1	22	10	24

primarily determined by mechanisms operating at the level of the eighth nerve. In some subjects, psychophysical recovery was slower than physiological recovery, suggesting that central factors may secondarily affect psychophysical measures of SPFM in some listeners.

In an earlier study, Brown and Abbas (1990) demonstrated an inverse correlation between recovery time constants obtained from physiological SPFM functions and scores on word and sentence recognition tasks, although a later report failed to confirm that relationship (Brown *et al.*, 1999). These interesting findings suggests that SPFM time constants could provide an index of peripheral auditory status in individual cochlear implant patients. To our knowledge, the relationship between psychophysical SPFM recovery characteristics and speech recognition has not yet been evaluated.

In summary, the existing literature indicates that SPFM is a potentially important phenomenon in electric hearing and warrants further investigation. The present study was designed to examine characteristics of psychophysical SPFM recovery functions, including the general form of the SPFM recovery function, the dependence of recovery function shapes on masker level, and the extent to which recovery characteristics vary across cochlear implant listeners and regions of the implanted array. Recovery functions were obtained from apical, middle and basal electrodes in each subject for masker levels ranging from 25 to 75% of the masker dynamic range, and were analyzed using an exponential model of recovery. Slopes of growth-of-masking functions derived from SPFM recovery functions were also evaluated.

## II. METHODS

### A. Subjects

Subjects were eight post-lingually deafened adults implanted with the Nucleus mini-22 electrode array and receiver/stimulator. Table I displays relevant information for each subject, including age at implantation, etiology of deafness, duration of hearing loss prior to implantation, duration of implant use prior to participation in the study, and performance on the NU-6 monosyllabic word test in quiet.

Psychophysical recovery functions were measured for each of three test electrodes per subject. Test electrodes were distributed across the electrode array, with one electrode near the apical end of the array, one electrode near the middle of the array, and a third electrode near the basal end of the array.<sup>1</sup> All subjects were stimulated in bipolar mode, using an electrode separation of 1.5 mm (BP+1 mode) or the narrowest separation greater than 1.5 mm that would allow maximum acceptable loudness to be achieved at realizable current amplitudes. Table II lists the specific electrode pairs evaluated in each subject and corresponding bipolar separations.

### B. Stimuli and procedures

#### 1. SPFM recovery functions

Experiments were controlled by a microcomputer connected through a parallel port to a specialized cochlear implant interface (Shannon *et al.*, 1990). Stimuli were single, biphasic current pulses with a per-phase duration of 200  $\mu$ s, and a delay between phases of 44  $\mu$ s. Figure 1 illustrates the stimulation protocol used to obtain SPFM recovery functions. As shown in the figure, a single "masker" pulse was presented first, followed at some time delay by a single

TABLE II. Test electrodes. Subject identifying code, test electrodes and their bipolar separations. Electrode numbers increase from apex to base (research electrode numbering system, denoted by an "r" before electrode number). Each electrode pair is referred to in the text by the higher-numbered (more basal) electrode. Bipolar separation refers to the distance between the active and reference electrodes in a given electrode pair. These separations were 1.5 mm (BP+1), 2.25 mm (BP+2), 3.0 mm (BP+3) or 3.75 mm (BP+4).

Subject code	Test electrodes (Bipolar separation)		
AGF	r12 (BP+2)	r16 (BP+1)	r21 (BP+1)
AMB	r06 (BP+2)	r12 (BP+2)	r20 (BP+2)
CJP	r05 (BP+2)	r12 (BP+2)	r19 (BP+2)
DAW	r04 (BP+1)	r17 (BP+1)	r21 (BP+3)
EJQ	r06 (BP+3)	r11 (BP+3)	r17 (BP+3)
GPB	r05 (BP+1)	r12 (BP+1)	r20 (BP+1)
JPB	r07 (BP+4)	r11 (BP+4)	r16 (BP+4)
RFM	r05 (BP+1)	r15 (BP+1)	r20 (BP+1)

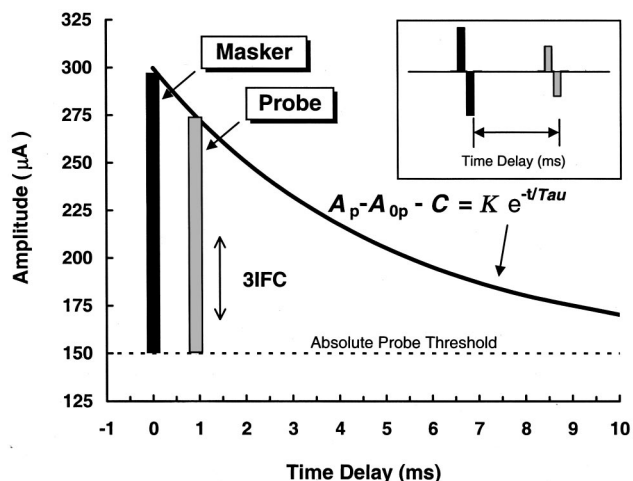


FIG. 1. Schematic diagram of the stimulus protocol used to measure single-pulse forward-masking recovery functions.

“probe” pulse. The current amplitude of the masker pulse was fixed, and for a particular time delay, the amplitude of the probe pulse was varied adaptively to determine masked threshold. By varying the time delay between masker and probe pulses in different adaptive tracks, a recovery function was defined. In this report, time delay (ms) is measured between masker offset and probe offset (Fig. 1 inset), masker and probe amplitudes are specified in microamperes ( $\mu\text{A}$ ) of current, and masked thresholds for the probe are specified in terms of threshold shift (TS) in  $\mu\text{A}$ , i.e., the amplitude difference between the masked threshold of the probe ( $A_p$ ) and the unmasked threshold of the probe in quiet ( $A_{op}$ ).<sup>2</sup>

## 2. Absolute thresholds and maximum acceptable loudness levels

Prior to obtaining recovery functions for a particular electrode, absolute detection threshold (THS) and maximum acceptable loudness level (MAL) were determined for the single-pulse stimuli. THS was measured with a 3-interval forced choice (3IFC) adaptive procedure similar to that used for measuring masked thresholds (described below). MAL was measured with an ascending method of limits procedure in which single pulses, presented at a rate of 2/s, were slowly increased in amplitude until the subject indicated that loudness had reached a “maximum acceptable” level. Estimates for two consecutive ascending runs were averaged to obtain a single measure of MAL. THS and MAL were measured at the start of each test session for the particular electrode to be evaluated in that session. Values reported here represent the average of all measures obtained across sessions.

## 3. Masked thresholds

Forward-masked thresholds were obtained using a 3IFC adaptive procedure. The masker pulse was presented in each of three listening intervals. The probe pulse was presented in one of the three intervals, chosen randomly from trial to trial, at some fixed time delay following the masker pulse. The subject’s task was to choose the “different” interval by pressing the appropriate button on a three-button computer mouse. Stimulus intervals were cued on a video monitor, and

correct-answer feedback was provided after each trial. The amplitude of the probe pulse was initially set 0.5 dB to 4 dB (depending on the dynamic range of the test electrode) above the anticipated masked threshold. For the first four reversals, probe level was altered according to a 1-down/1-up stepping rule, with step size equal to 1 dB (about 6 current step units {CSUs}).<sup>3</sup> These initial reversals quickly moved the adaptive procedure into the target region for masked threshold. After the fourth reversal, step size was reduced, typically to one-fourth of the initial step size, and a 3-down/1-up stepping rule was assumed. This stepping rule estimates the stimulus level corresponding to 79.4% correct discrimination (Levitt, 1971). Step size was constant for all remaining trials. Trials continued until a total of 12 reversals occurred. The mean of the final 8 reversals was taken as the masked threshold estimate.

Masked thresholds were determined in this manner for 9 time delays from 1 ms to 256 ms, in octave steps, to define a complete forward-masking recovery function. Each point on the recovery function was based on the average of 3 to 5 forward-masked threshold estimates. Data were obtained in sets, where a single set included one adaptive track at each time delay. Three to five sets were obtained with the order of time delays alternated for consecutive sets (short-to-long time delays alternated with long-to-short). This allowed any learning effects to be distributed across time delays. Most recovery functions were completed within a single test session. At the end of a session, absolute threshold for the probe pulse was re-measured to insure that no significant shifts in unmasked threshold had occurred due to auditory fatigue.

Recovery functions were obtained in this manner at several masker levels distributed across each electrode’s dynamic range. Four or five masker levels were assessed for electrodes with large dynamic ranges; fewer masker levels were assessed when dynamic ranges were small. Only 1 or 2 masker levels were tested in five electrodes. For one subject (AMB), three masker levels were tested per electrode but only one or two of these produced sufficient threshold shift to allow fitting with exponential functions.

## III. RESULTS

### A. Characteristics of individual SPFM recovery functions

#### 1. Exponential function fits

Least-squares regression procedures were used to fit individual recovery functions with the equation

$$(A_p - A_{op} - C) = K \cdot e^{-t/\tau}, \quad (1)$$

where  $A_p$  is the forward-masked threshold of the probe ( $\mu\text{A}$ ),  $A_{op}$  is the unmasked probe threshold ( $\mu\text{A}$ ),  $t$  is the masker-probe time delay (ms),  $\tau$  is the time constant of recovery from forward masking (ms), and  $K$  and  $C$  are constants. The constant  $C$  was included in Eq. (1) to accommodate residual masking (incomplete recovery) observed in some recovery functions at moderate or long masker-probe delays. Such residual masking is commonly observed in acoustic forward-masking experiments (Abbas and Gorga, 1981; Markman,

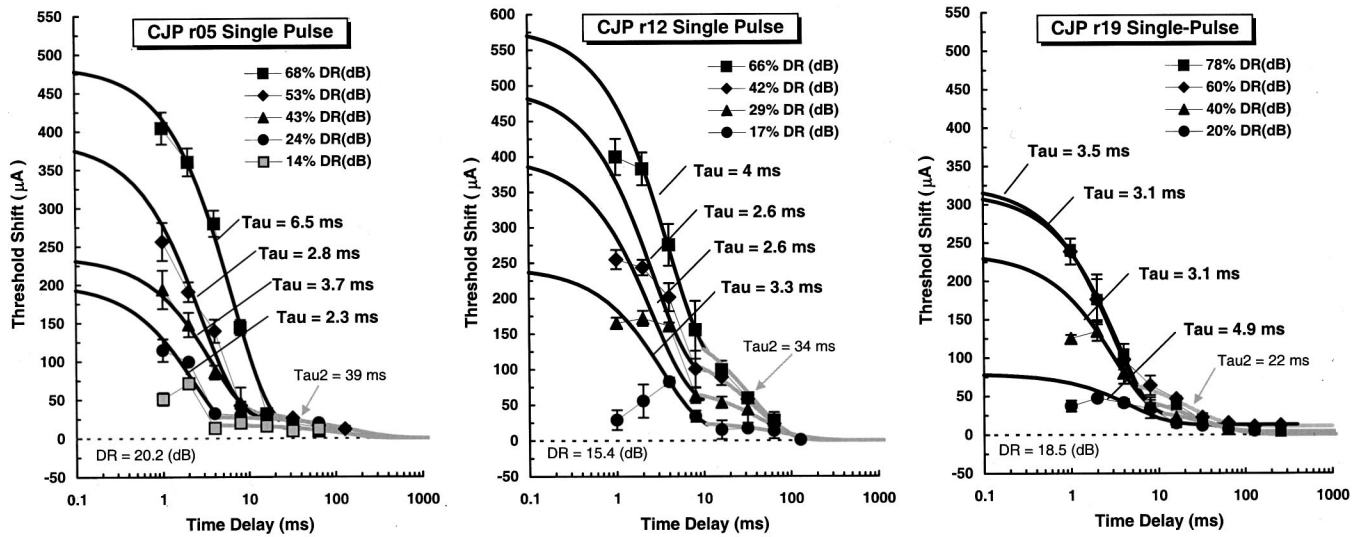


FIG. 2. Single-pulse forward-masking recovery functions as a function of the time delay between masker offset and probe offset. Data are from subject CJP, who demonstrated short time constants for the rapid-recovery process ( $\tau < 7$  ms) as well as relatively short time constants for the slow-recovery process. Each panel contains recovery functions for a single electrode (apical, middle, and basal electrodes, from left to right). Error bars indicate 1 standard deviation from the mean. The parameter is masker level, expressed in the legend as the percentage of the dynamic range available on each electrode. Dynamic range for each electrode is given within the panel. Time constants are indicated by  $\tau$  for each rapid-recovery function and by  $\tau_2$  for the slow-recovery function obtained at the highest masker level.

1989; Oxenham and Moore, 1995), but is not well understood.

As described below, many recovery functions in the present study exhibited two separate components, one at short time delays ( $t < 10$  ms) and the other at longer time delays ( $t > 10$  ms). In later descriptions of the data, these components are referred to as the “rapid” and “slow” recovery processes, respectively. Equation (1) was used to fit each process independently over the subset of time delays for which it appeared to dominate the overall recovery function. In most cases, the break-point between processes occurred at a time delay of about 10 ms. For convenience, fitting parameters for the rapid-recovery process are specified  $\tau$ ,  $K$ , and  $C$ , and fitting parameters for the slow-recovery process are specified  $\tau_2$ ,  $K_2$ , and  $C_2$ .

## 2. Rapid- and slow-recovery processes

SPFM recovery functions for one subject (CJP) are shown in Fig. 2. These functions are typical of functions obtained from five of the eight subjects tested in the present study (CJP, DAW, EJQ, JPB, and RFM). Several general characteristics are demonstrated by recovery functions in the left panel of Fig. 2, which were obtained from CJP’s apical test electrode (r05). First, note that two distinct recovery processes are evident, a rapid-recovery process at short time delays ( $< 10$  ms), and a slower process at longer time delays ( $> 10$  ms). Both the rapid and slow components are well described by the exponential recovery process given in Eq. (1). Time constants for the rapid process ( $\tau$ ) range from 2.3 ms to 6.5 ms for masker levels ranging from 14 to 68% of dynamic range. This particular electrode has a large dynamic range (20.2 dB); thus, masker levels encompass a large range of current amplitudes (183–576  $\mu\text{A}$ ). Only a small amount of masking is involved in the slow-recovery process, and there is almost no residual masking at the longest time de-

lays. Fitted time constants for the slow-recovery process ( $\tau_2$ ) varied from approximately 40 ms to 120 ms for different masker levels. Only the time constant (39.5 ms) for the highest masker level (68% DR) is indicated in the figure.

The center and right panels of Fig. 2 show corresponding data for subject CJP’s middle and basal test electrodes, respectively. Note that the amount of masking for the slow-recovery process varies across electrodes, even though all three electrodes show similar time constants (3–6 ms) for the rapid-recovery process. This suggests that the rapid- and slow-recovery processes are independent or only weakly related, and may stem from different physiological mechanisms.

## 3. Facilitation at short time delays

For most electrodes, the rapid-recovery process was well described by a decaying exponential function defined by Eq. (1); however, clear departures were sometimes observed. The most common departure was a nonmonotonicity at short time delays (1–2 ms) that resulted in masked thresholds that were lower than those predicted by the exponential function. We refer to this nonmonotonic behavior as “facilitation.” As discussed later, facilitation could stem from the same peripheral phenomenon underlying nonmonotonicities in 8th nerve SPFM recovery functions (Stypulkowski and van den Honert, 1984; Miller *et al.*, 1993), or could reflect subjects’ use of loudness cues at very short masker-probe delays. Facilitation is demonstrated by CJP on electrode r05 at the lowest masker level (left panel in Fig. 2), on electrode r12 at all masker levels but more so at the lower levels (center panel), and on electrode r19 at the two lowest masker levels (right panel). Nineteen of the twenty-four electrodes tested in the present study exhibited facilitation at the shortest time delays for one or more masker levels, with the largest facilitation usually occurring at the lowest masker levels. When

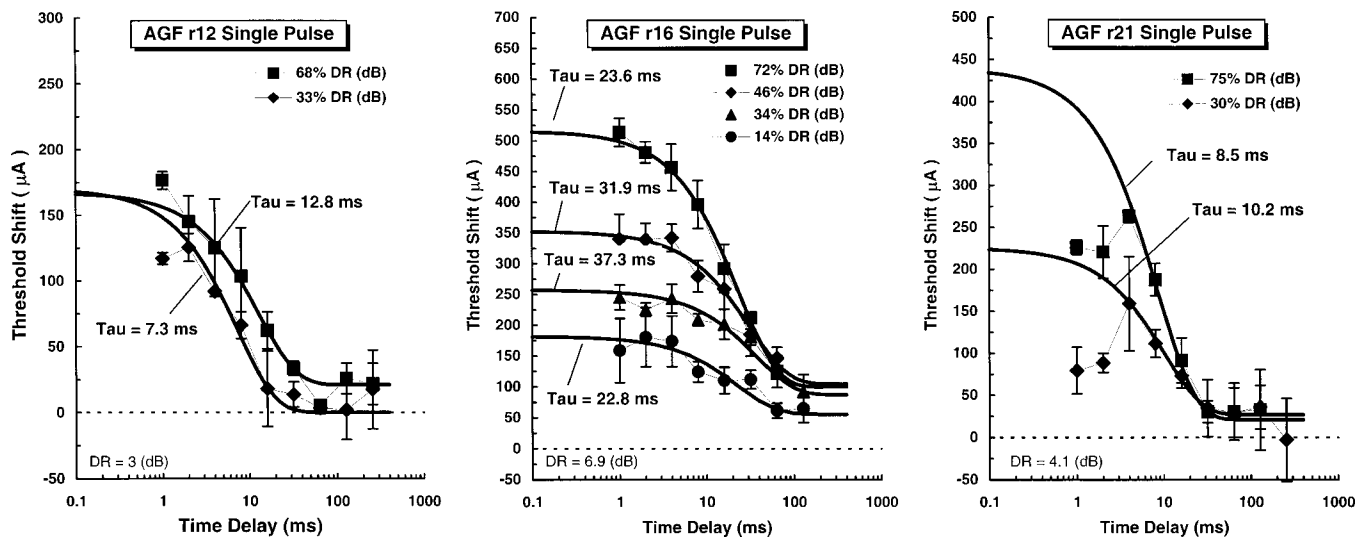


FIG. 3. Single-pulse forward-masking recovery functions, as in Fig. 2. Data for subject AGF, who demonstrated long time constants for the rapid-recovery process ( $>7$  ms), and no clear slow-recovery process. Residual masking is evident at long time delays, which may reflect a slow-recovery process with an exceptionally long time constant.

facilitation was clearly present, masked thresholds at the shortest time delays were excluded from exponential curve fits. This occasionally left too few remaining data points at short masker-probe delays to permit meaningful fits to be obtained, as was the case for electrode CJPr05 at the lowest masker level.

#### 4. Atypical functions

Although five of eight subjects demonstrated recovery functions similar to those shown in Fig. 2, three subjects demonstrated distinctly different SPFM recovery characteristics. Figure 3 shows the recovery functions for one such subject, AGF, who demonstrated unusually long time constants for the rapid-recovery process, especially on his middle electrode, r16 ( $\tau=23\text{--}37$  ms). Slow-recovery processes were not evident in this subject's data; however, electrode r16 showed substantial residual masking at long time delays. This could indicate that a slow-recovery process existed, but was not well defined within the range of time delays evaluated. Note that considerable facilitation was observed on r21. Also note that subject AGF has very poor word recognition (Table I), suggesting a possible relationship between prolonged SPFM time constants and poor speech recognition.

Figure 4 shows data for a second subject, GPB, who exhibited atypical recovery functions. GPB's time constants for the rapid-recovery process were not unusual (2–7 ms); however, time constants for the slow-recovery process were prolonged ( $>200$  ms) for all three electrodes, and there was substantial residual masking present at long time delays for the apical and middle electrodes (r05 and r12). Note that strong facilitation was evident for both the apical and basal electrodes (r05 and r20) and that these electrodes exhibited extremely small dynamic ranges (3.2 and 2.3 dB, respectively). Also notice that there is a clear demarcation between rapid- and slow-recovery processes on the middle electrode (r12).

Figure 5 shows data for the third subject who demonstrated unusual recovery functions, subject AMB. The notable aspect of these functions is the amount of facilitation demonstrated at low masker levels and the fact that masked thresholds were clearly lower than unmasked thresholds for some conditions involving low masker levels and short time delays. Time constants for the rapid-recovery process were similar to those for CJP and other "typical" subjects. A second recovery process was evident on the middle electrode (r12) at the highest masker level, but there was no evidence of a second recovery process on electrodes r06 or r20, or at lower masker levels on r12.

#### B. Growth of masking

If an exponential model with a level-independent time constant is appropriate for describing the single-pulse recovery process, then the model should accurately predict the rate at which single-pulse forward masking grows with masker level at all time delays. To evaluate characteristics of growth of masking (GOM) for the rapid-recovery process, parameter  $K$  in Eq. (1) was expressed as a linear function of masker sensation level ( $A_m - A_{0m}$ ), as follows:

$$K = b + n \cdot (A_m - A_{0m}). \quad (2)$$

Substituting Eq. (2) for  $K$  in Eq. (1) yields the following:

$$(A_p - A_{0p} - C) = [b + n(A_m - A_{0m})] \cdot e^{-t/\tau}. \quad (3)$$

This shows that for a time delay of  $t=0$  ms, the growth rate of masking is equal to  $n$ , and the sensitivity to masking is equal to  $b$ . For other values of  $t$ , Eq. (3) shows that the rate of growth of masking is inversely related to  $\tau$ . Growth of masking slopes were evaluated for several values of  $t$  in order to determine if the expected dependence of growth rate on  $\tau$  was actually reflected in the data.

The y-intercept,  $K$  (value at  $t=0$ ), of recovery functions fitted with Eq. (3) provides a measure of response growth rate that is independent of the time constant. In Fig. 6(A),

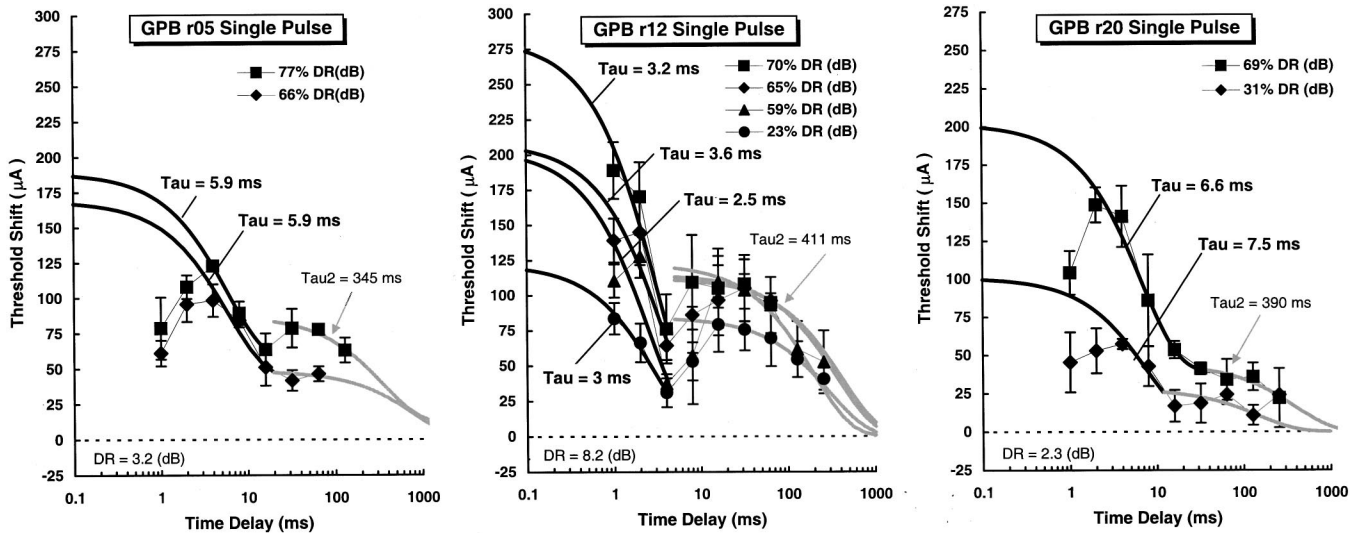


FIG. 4. Single-pulse forward-masking recovery functions, as in Fig. 2. Data for subject GPB, who demonstrated typical, short time constants for the rapid-recovery process, but demonstrated unusually large amounts of masking at longer time delays together with extended time constants for the slow-recovery process.

values of  $K$  for subjects' rapid-recovery processes are plotted as a function of masker level in  $\mu\text{A}$  to obtain growth-of-masking (GOM) functions at a time delay of 0 ms. A solid line with a slope of 1.0 is shown for reference. Data for most electrodes can be described by straight line functions with unity slopes over a wide range of masker levels, but in some cases the measurement detail (only two data points) is insufficient to obtain a valid determination of slope. Although the individual GOM functions in Fig. 6(A) tend to have similar slopes, their origins vary considerably due to differences in absolute threshold. Such differences are reduced by expressing masker level relative to absolute threshold, in sensation-level units, as shown in Fig. 6(B). Each GOM function in Fig. 6(B) was fitted with Eq. (3) to determine its slope,  $n$ , and sensitivity constant,  $b$ . The average slope,  $n$ , across electrodes was 1.01 and the average sensitivity constant,  $b$ , was  $66 \mu\text{A}$ .<sup>4</sup> The average slope indicates that effective masking

due to a single-pulse masker tends to grow linearly with the sensation level of the masker (in  $\mu\text{A}$ ). The average sensitivity constant suggests, by extrapolation, that single-pulse forward masking begins when masker amplitude is slightly below absolute threshold.

For time delays greater than 0 ms, Eq. (3) predicts that GOM slopes will be shallower than the unity slope observed at zero time delay, with slopes depending both upon the time delay ( $t$ ) and the time constant for recovery ( $\tau$ ). Figures 6(C) and (D) show threshold shifts predicted by the fitted recovery curves at time delays of 2 and 5 ms. In these panels, both threshold shift and masker level are expressed as a percentage of the dynamic range (%DR) available on the test electrode. This normalization, accomplished by dividing both threshold shift and masker level by the dynamic range in  $\mu\text{A}$ , makes changes in GOM slope more apparent across electrodes with widely different dynamic ranges.

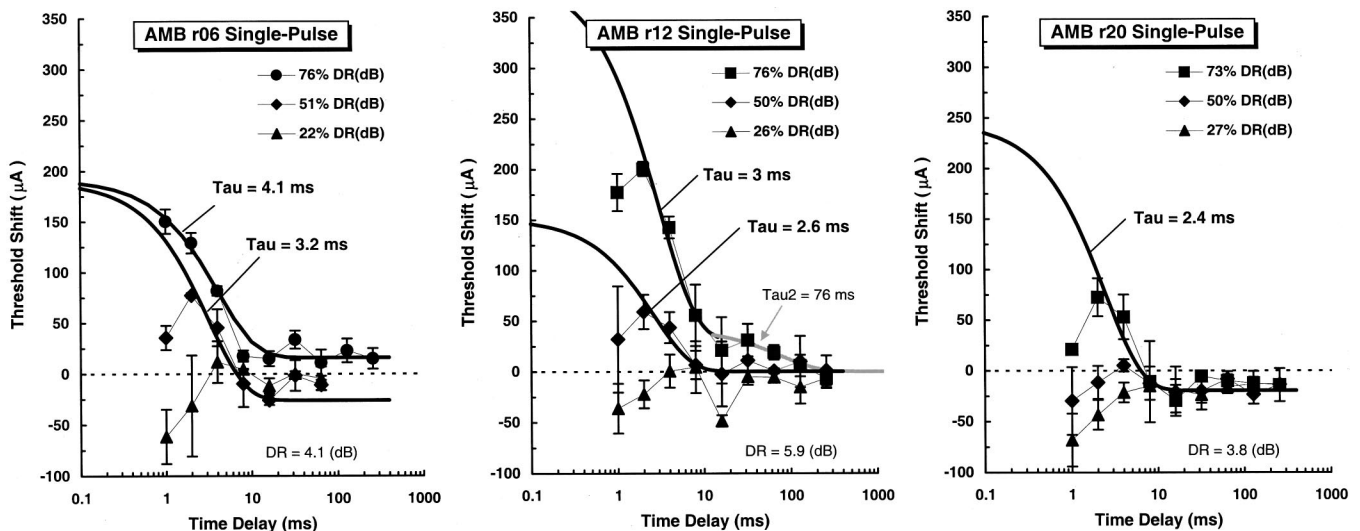


FIG. 5. Single-pulse forward-masking recovery functions, as in Fig. 2. Data for subject AMB, who demonstrated typical, short time constants for the rapid-recovery process, but demonstrated particularly large facilitation effects at the shortest time delays, especially for the lower two masker levels. The facilitation effect can be seen as an improvement in masked threshold as time delay becomes shorter than 2–4 ms, depending upon masker level.

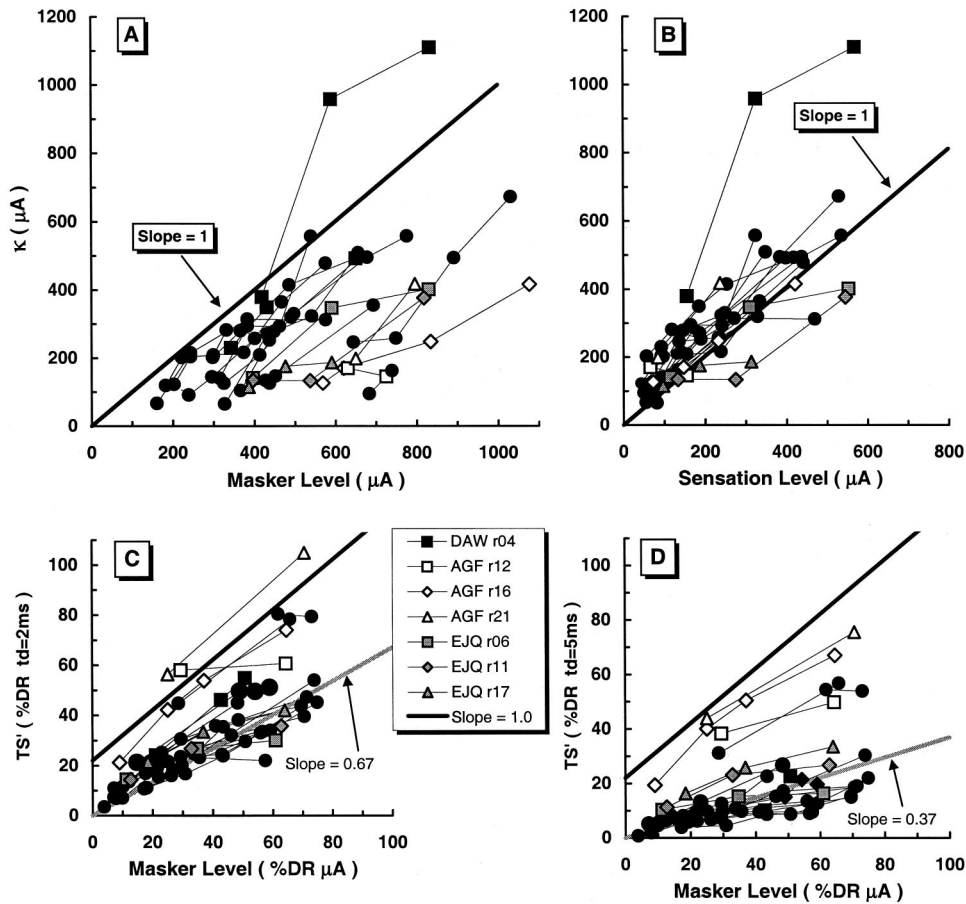


FIG. 6. Amount of masking as a function of masker level. Amount of masking (threshold shift in  $\mu\text{A}$ ) at a time delay of 0 ms was obtained from the intercepts ( $K$ ) of exponential fits to the rapid-recovery process of single-pulse forward masking. *Panel (A)*: Amount of masking ( $K$ ) as a function of the physical masker level in  $\mu\text{A}$ . A slope of 1.0 is shown by the wide line. *Panel (B)*: Amount of masking ( $K$ ) as a function of the relative level of the masker above absolute threshold. The average slope of the growth of masking at  $t_d=0$  ms is shown by the wide line. *Panel (C)*: Amount of masking ( $TS'$  in % DR) calculated for a time delay of 2 ms, as a function of masker sensation level expressed as % DR ( $\mu\text{A}$ ). The average slope of the growth of masking at  $t_d=2$  ms (0.67) is shown by the gray line. A slope of 1 is shown by the black line. *Panel (D)*: Amount of masking ( $TS'$  in % DR) calculated for a time delay of 5 ms, as a function of masker sensation level expressed as % DR ( $\mu\text{A}$ ). The average slope of the growth of masking at a time delay of 5 ms (0.37) is shown by the gray line. A slope of 1 is shown by the black line.

Average GOM slopes were 0.67 at  $t=2$  ms [panel (C)] and 0.37 at  $t=5$  ms [panel (D)]. Values of  $\tau$  that would yield these average slopes were computed to be 5.1 ms at both time delays, which is close to the average measured  $\tau$  of 5.5 ms. Conversely, this average value of  $\tau=5.5$  ms predicts GOM slopes of 0.69 and 0.40, respectively, at time delays of 2 and 5 ms [Eq. (3)]. These predicted slopes are very close to the average slopes of 0.67 and 0.37 shown in Figs. 6(C) and (D). The similarity of predicted and measured values indicates that the exponential recovery process adequately describes the data. Notice that the subject with the longest time constant, AGF, exhibits the steepest GOM slope and the greatest amount of threshold shift at 2 and 5 ms [Figs. 6(C) and (D)]. The steep GOM slope is a direct consequence of this subject's prolonged time constant, but the greater amount of masking seems to be related to a relatively narrow dynamic range. This suggests the possibility that subjects with narrow dynamic ranges may be more susceptible to prolonged recovery from SPFM than those with wider dynamic ranges.

### C. Group tendencies in SPFM recovery functions

#### 1. Summary of fitting parameters

Table III summarizes recovery function parameters for all subjects and electrodes, for SPFM data obtained at the highest masker level ( $>60\%$  DR). For each test electrode (denoted by research electrode number, rEL), threshold and dynamic range for the single-pulse probe (or masker) stimulus are shown, together with fitting parameters  $\tau$ ,  $K$ , and  $C$

for the rapid-recovery process. Exponential fits to the initial rapid-recovery process were excellent, as evidenced by coefficients of determination ( $r^2$ ) that averaged 0.98 across all three masker levels ( $-2$  s.e.=0.965). Values for  $\tau_2$  are shown for 19 (out of 24) electrodes that clearly demonstrated a second slow-recovery process. Exponential fits to the slow-recovery process were not as good, as evidenced by coefficients of determination that averaged 0.82 across all three masker levels ( $-2$  s.e.=0.757). Table III also shows the relative amounts of masking present at a time delay of 2 ms, which were estimated from the fitted recovery functions. Amount of masking is expressed in terms of a percentage of the dynamic range existing on each electrode (%DR).

#### 2. Masker level effects

The exponential model used to describe these data resulted in time constants for the rapid-recovery process ( $\tau$ ) that were independent of masker level. As shown in Fig. 7, values for  $\tau$  varied considerably across subjects, from 1.5 ms to 37.3 ms, but for individual electrodes did not vary systematically with masker level. Thus, the exponential recovery model defined by Eq. (1), with a level-independent time constant, appears to adequately describe the SPFM recovery process. The average value of  $\tau$  across all subjects and electrodes was 5.5 ms. Only two subjects (AGF and EJQ) consistently demonstrated time constants that were longer than 7 ms, the value 2 standard errors above the mean (dashed line in Fig. 7). As will be discussed later, these two subjects also performed poorest on the NU-6 word recogni-

TABLE III. Recovery function parameters. Parameters obtained from exponential fits to single-pulse forward-masked thresholds for each electrode at the highest masker level ( $L_m > 60\%$  DR). (See text.)

Subject rEL	THS (dB $\mu$ A)	DR (dB)	Lm (% DR)	$\tau$ (ms)	$\kappa$ ( $\mu$ A)	C ( $\mu$ A)	$r^2$	$\tau_2$ (ms)	C2 ( $\mu$ A)	%DR (td=2ms)
AGF r12	55.1	3.1	68.3%	12.8	146.2	21.0	0.995		0.0	61
AGF r16	56.3	6.0	71.9%	23.6	416.0	100.0	0.990		100.0	74
AGF r21	55.0	4.1	75.2%	8.5	417.9	21.1	0.997		0.0	105
AMB r06	52.9	4.5	75.6%	4.1	176.0	13.0	0.990		0.0	41
AMB r12	51.0	6.3	75.8%	3.0	361.1	31.0	0.984	75.7	0.0	58
AMB r20	53.6	4.1	72.5%	2.4	265.6	-19.5	0.943		-19.5	34
CJP r05	42.6	18.6	67.9%	6.5	478.3	7.0	0.994	39.5	0.0	35
CJP r12	47.3	13.5	66.4%	4.0	492.5	89.5	0.999	34.2	0.0	45
CJP r19	40.5	18.8	78.2%	3.5	311.9	4.0	1.000	25.6	4.0	22
DAW r04	48.4	14.4	69.3%	3.4	1110.0	0.0	0.994	50.0	0.0	55
DAW r17	46.7	11.2	70.8%	1.7	556.8	23.0	0.997	55.8	0.0	34
DAW r21	47.6	12.4	82.3%	2.0	557.3	95.4	0.999	43.8	13.1	40
EJQ r06	48.8	12.6	75.5%	4.7	402.1	10.2	0.989	75.5	0.0	30
EJQ r11	48.7	12.4	76.7%	10.4	377.2	0.0	0.956	98.5	0.5	36
EJQ r17	48.9	8.8	74.3%	9.4	186.7	55.0	0.949	87.7	24.0	42
GPB r05	50.0	3.4	76.7%	5.9	134.4	23.0	1.000	345.3	0.0	79
GPB r12	44.0	9.1	70.5%	3.2	282.4	0.0	0.949	411.0	0.0	51
GPB r20	55.6	2.5	69.0%	6.6	162.8	39.0	0.989	389.5	0.0	78
JPB r07	47.8	6.5	76.7%	2.4	252.6	9.3	0.973	83.9	0.0	44
JPB r11	48.2	11.5	70.5%	2.0	491.4	57.2	0.999	23.5	1.6	33
JPB r16	49.8	8.2	79.7%	1.8	508.6	60.0	0.983	14.7	2.1	47
RFM r05	54.0	8.0	78.1%	2.6	672.3	18.5	1.000	43.1	0.0	44
RFM r15	44.2	11.4	84.6%	2.6	319.7	49.2	0.978	74.6	...	45
RFM r20	51.2	7.0	80.7%	5.2	355.0	0.0	0.994	48.8	0.4	54

tion test (see Table I). One subject (GPB) demonstrated time constants close to 7 ms on one electrode, but time constants for his other two electrodes were closer to the mean.

### 3. Effects of electrode location

To examine whether recovery function parameters differed for electrodes located in the apical, middle, or basal regions of the electrode array, single factor repeated-measures ANOVAs were performed for the measures  $\tau$ ,  $K$ ,  $\tau_2$  and threshold shift at  $t=2$  ms and  $t=5$  ms. None of the resulting  $F$  ratios approached statistical significance. This indicates that neither the recovery from SPFM nor the amount of masking at any time delay varied consistently according to electrode region. Repeated-measures ANOVAs similarly showed that neither absolute threshold nor dynamic range varied systematically with electrode location.

### 4. Correlations among fitting parameters

Comparisons were made between measures of dynamic range (DR), absolute threshold (THS), maximum acceptable loudness level (MAL), and parameters of the SPFM recovery functions ( $\tau$ ,  $K$ ,  $C$ ,  $\tau_2$ ,  $K_2$ , and threshold shift at different delay times). There was a significant negative correlation ( $R = -0.99$ ;  $p < 0.01$ ) between DR and THS for the basal electrodes, but that relationship was weaker for the middle and apical electrodes ( $R = -0.63$  and  $-0.78$ , respectively). Correlations between DR and MAL were positive but not significant for apical, middle, and basal electrodes ( $R = 0.71$ ,  $0.10$ , and  $0.57$ , respectively). This suggests that larger dynamic ranges are primarily determined by lower THS levels rather than higher MAL levels. There were no significant relations among the other parameters. The lack of

significant correlations between parameters of the rapid-recovery process ( $\tau$ ,  $K$ ,  $C$ ) and the slow-recovery process ( $\tau_2$ ,  $K_2$ ) supports our earlier speculation that these two processes operate independently and are governed by different physiological mechanisms.

### 5. Correlations with word recognition scores

As mentioned earlier, Brown *et al.* (1990) demonstrated an inverse correlation between recovery time constants measured with an electrophysiological SPFM procedure and

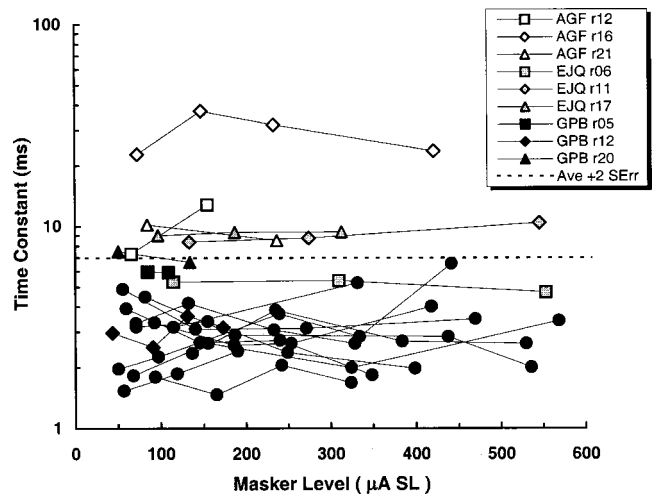


FIG. 7. Time constants for the rapid-recovery process as a function of masker level. Time constants were obtained from exponential fits of single-pulse forward-masking recovery functions. The dashed line indicates two standard errors above the mean. Time constants for outlying subjects are identified in the legend with separate symbols, those for the rest of the subjects are plotted as filled circles.



speech recognition scores in a group of 10 users of the Ineraid cochlear implant. To determine whether a similar relationship existed for the present subjects, NU-6 word recognition scores (Table I) were compared with SPFM time constants for subjects' apical, middle, and basal electrodes (Table III). An inverse relationship between word recognition and  $\tau$  was observed for all electrode locations; however, a statistically significant correlation coefficient was obtained only for the basal location ( $R = -0.89$ ,  $p < 0.01$ ). A scatterplot of the basal electrode data is shown in Fig. 8(A). Comparable data are replotted from Brown *et al.* (1990) in Fig. 8(B).

#### IV. DISCUSSION

##### A. Exponential recovery process

An important finding of this study was that recovery from psychophysical single-pulse forward masking can be accurately described by recovery processes in which the amount of threshold shift produced by a masker pulse recovers exponentially in time. Two recovery processes were observed, a rapid-recovery process and a slow-recovery process. Our findings indicate that the rapid-recovery process was dominant and could be measured from all test electrodes. The rapid-recovery process required only a single time constant to account for recovery data obtained over a wide range of masker amplitudes. The average rapid-recovery time constant across 24 electrodes in eight subjects was 5.5 ms, with a standard error of 0.75 ms. This means that approximately 95% of electrodes in a similar cochlear implant population would be expected to demonstrate time constants shorter than 7 ms. The slow-recovery process was inconsistent across subjects and electrodes, with time constants ranging from 20 to 400 ms, and in some cases was not evident at all.

In this study, threshold shift was specified in terms of microamperes of current. That is, the effect of the masker was specified as a difference in  $\mu A$  between the forward-masked threshold and absolute threshold. This differs from the traditional approach in acoustic hearing that specifies threshold shift as a ratio of masked threshold to absolute threshold, i.e., in decibels. In electric hearing, dynamic ranges are small and, therefore, threshold shift in decibels is also small ( $< 10$  dB). This predicts that good exponential fits can be obtained whether threshold shift is expressed in decibels or in  $\mu A$ . In fact, refitting the present data using decibels of threshold shift produced similar time constants with only slightly poorer fits. Even so, it seems appropriate to specify threshold shift in terms of linear  $\mu A$  of current, since the compressive nonlinearities in acoustic hearing are a product of cochlear processes that are absent in electric hearing.

Loudness matches obtained in listeners with acoustic hearing in one ear and electric hearing in the opposite ear suggest that linear changes in  $\mu A$  of current are proportional to decibels of acoustic sound pressure (Eddington *et al.*, 1978; Zeng and Shannon, 1992). Thus, the use of linear  $\mu A$  of current as the input to a more central adaptation mechanism in electric hearing is consistent with the use of decibels as the input to the same central adaptation mechanism in

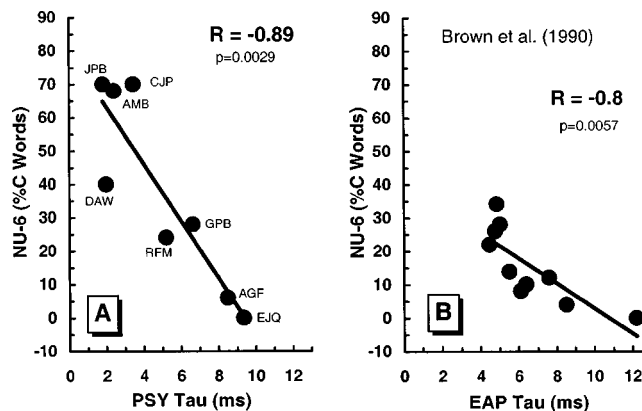


FIG. 8. Scattergrams of speech scores and time constants ( $\tau$ ) of SPFM recovery functions. Panel (A) Data for basal electrodes of subjects in the present study, for whom time constants were measured using a psychophysical (PSY) SPFM procedure. Panel (B) Data for subjects from Brown *et al.* (1990), for whom time constants from monopolar basal electrodes of an Ineraid cochlear implant were obtained using an electrically evoked action potential (EAP) measure of SPFM recovery.

acoustic hearing (Duifhuis, 1973; Nelson and Freyman, 1987; Nelson and Pavlov, 1989).

Also note that we chose to describe the recovery process as an *effect* of the masker that recovers over time and not as a decay in the physical amplitude of the masker. This is because the recovery curves all tended to asymptote at absolute threshold. None of the rapid- or slow-recovery curves were well fit using an equation that described exponential decay as a function of masker amplitude.

The exponential recovery process used to fit SPFM recovery curves, described by Eq. (3), is essentially identical to the recovery process used by Brown *et al.* to describe their physiological (1990, 1996) and psychophysical (1996) recovery curves. The principal difference is that Brown *et al.* normalized their functions to the masked threshold at some short time delay, thereby eliminating differences in the amount of masking across subjects (normalization does not affect time-constant estimates), and they did not include a constant ( $C$ ) to describe residual masking at longer time delays. Time constants (inverses of reported recovery slopes) for their physiological data ranged from 4.5 to 12.2 ms across 10 subjects. Time constants for their psychophysical data for six electrodes in four subjects, estimated with our fitting procedures, ranged from 2.2 to 14.7 ms.

In summary, both the form of the recovery curve described by Eq. (3) and the range of time constants obtained across subjects and electrodes in the present study, are consistent with data from previous physiological and psychophysical studies. About three-fourths of recovery functions reported in existing studies have time constants shorter than 7 ms, roughly similar to eighth-nerve refractory time constants measured in normal and acutely deafened ears. The remaining psychophysical functions have time constants longer than 7 ms, perhaps indicating unusual amounts or types of auditory nerve degeneration.

##### B. GOM slopes

GOM slopes in this study decreased with time delay as expected in an exponential recovery process. Our analyses

indicate that effective masking (amount of masking at zero time delay) grows linearly with masker sensation level expressed in  $\mu\text{A}$ , and that GOM slope is determined by the recovery time constant,  $\tau$ , and the time delay,  $t$ . This finding, that GOM slopes can be predicted from the recovery time constant, supports the validity of an exponential model for describing SPFM recovery.

### C. Residual threshold shift and the slow-recovery process

One of the differences between previous work and the present study is our use of a  $C$  constant to reflect residual threshold shift and improve exponential fits to the SPFM recovery curves. As indicated in Table III,  $C$  constants for the rapid-recovery process ranged from 0 to 100  $\mu\text{A}$ . These constants were typically associated with a clearly defined slow-recovery process (e.g., CJP in Fig. 2). In some cases, however, substantial residual masking existed but no second recovery process was apparent, perhaps because sufficiently long time delays were not evaluated (e.g., AGF in Fig. 3). Examination of the Brown *et al.* (1996) psychophysical recovery functions suggests that the use of an additive constant might have improved some of their exponential fits (e.g., IS24 3–4 in their Fig. 12). This was not true of their EAP (electrically evoked action potential) recovery functions, however, suggesting that threshold shifts at long masker-probe time delays (residual masking or a well-defined slow-recovery process) represent some form of adaptation originating central to the eighth nerve. Further evidence for this is provided by the Brown *et al.* (1996) finding that psychophysical SPFM functions exhibited slower recovery than EAP SPFM functions in some subjects at time delays longer than 2–5 ms. Although procedural differences in psychophysical and EAP forward-masking procedures could contribute to such differences, both their findings and ours are consistent with the existence of two recovery processes, an initial rapid process associated with eighth-nerve relative refractoriness, and a second slower process that may be associated with more central adaptation.

### D. Level-independent time constants

The present study represents the first thorough examination of the level dependence of the recovery time constant in SPFM. From Fig. 7 it is clear that there were no systematic changes in time constant across masker levels, either within or across subjects and electrodes. That is, time constants in this study were level independent. A similar finding was recently reported by Hong *et al.* (1998), who found that recovery time constants were unaffected by masker level as long as masker level exceeded probe level. This was generally the case in our study, and in those instances where probe level did exceed masker level the differences were small. Thus, findings of the two studies are consistent. Note, however, that it would not be surprising to observe a masker-level effect under conditions in which probe level substantially exceeded masker level. In that circumstance, the probe could excite a significantly larger population of auditory nerve fibers than the masker and recovery functions might be less

affected by the refractory characteristics of individual neurons excited by the masker than by the recruitment of new fibers by the probe. Under more typical conditions in which masker level exceeds or is similar to probe level, our data indicate that an exponential recovery process with a level-independent time constant adequately describes the rapid process of SPFM recovery.

### E. Electrode location effects

In the present study, SPFM recovery parameters did not vary systematically with electrode location, suggesting that underlying neural characteristics did not vary consistently with cochlear location across subjects. This finding agrees with Brown's findings for EAP recovery functions (Brown *et al.*, 1996). Note, however, that for individual subjects in the present study, rapid-process time constants sometimes showed large differences for apical, middle and basal test electrodes (Table III). Four subjects exhibited time constants that were 2–2.7 times larger on one electrode than another (AGF, GPB, RFM, and EJQ), suggesting local differences in neural survival along the cochlear partition. Additional evidence for local effects of neural survival is provided by a recent comparison of EAP recovery curves obtained with monopolar and bipolar stimulation (Brown *et al.*, 1996). Monopolar stimulation produced nearly identical recovery functions in a group of nine subjects, whereas bipolar stimulation produced more variable function shapes in a group of 13 subjects (see their Fig. 8). One interpretation of this finding is that bipolar stimulation sampled more discrete regions of the cochlear partition than monopolar stimulation, thereby allowing local differences in neural survival to have a greater influence on results.

### F. Comparison with eighth-nerve recovery functions

Examination of physiological data from animals supports the hypothesis that the rapid-recovery process seen in human SPFM functions reflects refractory properties of the eighth-nerve response. Stypulkowski and van den Honert (1984) measured EAP recovery functions in normal-hearing and short-term deafened cats, and identified two components of the EAP on the basis of latency-intensity characteristics: The shorter-latency  $N0$  component was thought to arise from stimulation of auditory nerve fibers' central processes (axons), whereas the longer-latency  $N1$  component was thought to arise from fibers' peripheral processes (dendrites). Refractory functions were examined for  $N1$  responses in normal-hearing and ototoxically-deafened animals who were presumed to have normal dendrites and axons, and for  $N0$  responses in laminectomized animals who were presumed to have functional axons but no dendrites. Both  $N1$  and  $N0$  recovery functions showed complete or near-complete recovery at masker-probe delays of 4 ms, consistent with recovery time constants of about 2–3 ms. Miller *et al.* (1993) identified two wave I components in the guinea pig EABR, analogous to the  $N0$  and  $N1$  responses studied by Stypulkowski and van den Honert (1984). Recovery was significantly faster for wave Ia (similar to  $N0$ , axonal stimulation) than for wave Ib (similar to  $N1$ , dendritic stimulation), but exponential time

constants for both waves were always less than 5 ms. Recovery functions for short-term deafened animals in the Miller *et al.* study were similar to those in normal-hearing animals, but showed greater variability across individuals. Zhou *et al.* (1995) measured EABR recovery functions in mice with myelin-deficient auditory nerve fibers. The myelin-deficient mice demonstrated slightly but significantly slower recovery than normal controls; however, recovery time constants were again about 2–3 ms for both myelin-impaired and normal animals.

The similarity of SPFM time constants in normal and short-term deafened animals, as well as most human subjects, suggests that recovery characteristics at the level of the eighth nerve are relatively insensitive to deafness-related changes in fiber morphology and density. As discussed below, an important exception to this may occur in the case of long-term deafness. The human psychophysical data do not allow differentiation of axonal versus dendritic excitation mechanisms, as there are not clear differences among functions with time constants less than 5 ms. However, the distribution of psychophysical time constants across electrodes and subjects (mean 5.5 ms, with a standard error of 0.75 ms) is broader than that seen in animals (typical range 2–3 ms). This could imply that the proportion of neural responses stemming from axonal versus dendritic excitation varies across subjects and electrodes, and that SPFM functions with the shortest time constants involve only axonal excitation.

### G. Extended time constants and long-term deafness

Most of Brown and Abbas' subjects (Brown *et al.*, 1990; Abbas and Brown, 1991; Brown *et al.*, 1996) evaluated with physiological and psychophysical measures of SPFM showed complete recovery at time delays of 4–6 ms ( $\tau < 5$  ms), consistent with animal data described above. However, a few showed noticeably slower recovery ( $\tau > 10$  ms), similar to that shown psychophysically by subject AGF in the present study. It is possible that prolonged recovery times are indicative of severe neural degeneration associated with long-term deafness. Information regarding individual subjects' duration of deafness is not provided in Brown and Abbas' studies; however, our subject AGF was profoundly deaf for 25 years prior to cochlear implantation, far longer than other subjects in this study. Subject AGF was also the oldest of our group (79 years), suggesting that age could be another factor contributing to prolonged recovery.

Physiologic factors that could account for prolongation of SPFM time constants in long-term deafness involve the recovery time constants of individual auditory nerve fibers and the density of residual neurons in the region of electrical stimulation. Recovery rates of individual fibers affect the likelihood that fibers responding to the masker pulse will respond again to the probe pulse at short time delays. In subjects with long-term deafness, it is conceivable that demyelination of fibers' axonal processes (Leake and Hradek, 1988) or reduced fiber diameters could prolong individual fiber time constants (Paintal, 1966), thereby contributing to prolonged SPFM time constants. Neural density is likely to influence the proportion of stimulated fibers that respond to the masker and are in a refractory state when the probe pulse

occurs. The proportion of refractory fibers should vary inversely with the time constants measured in SPFM and, at least intuitively, should vary inversely with neural density. Thus, reduced neural density may also be associated with prolongation of SPFM time constants. A number of human and animal studies have shown that the density of functional auditory neurons decreases following deafness, and that the number of viable fibers may be severely reduced in some cases of long-term deafness. Subjects with severe neural depletion would also be those most likely to exhibit morphological changes resulting in prolonged recovery for individual fibers, suggesting that both factors may operate in tandem to prolong SPFM time constants. Subject EJQ's hearing loss was attributed to mumps, one of several viruses that can cause severe cochlear damage (Schuknecht, 1974) and associated neural degeneration. EJQ also demonstrated prolonged rapid-recovery constants for two electrodes ( $\tau$ 's more than two standard errors above the mean), consistent with the idea that prolonged time constants are indicative of neural degeneration. An evaluation of SPFM recovery functions in a larger population of cochlear implantees with varying durations of deafness and etiologies of hearing loss is needed to further address this possibility.

### H. Facilitation

The effect that we refer to as psychophysical facilitation was observed for nearly all electrodes evaluated in the present study at one or more masker levels. In general, facilitation was stronger at lower masker levels than at higher masker levels; however, masker level did not have a systematic effect on the amount of facilitation observed for individual electrodes.

It is interesting that nonmonotonicities similar to the facilitation seen here exist in the eighth-nerve measures of SPFM described earlier, suggesting that facilitation may reflect some physiological phenomenon at the level of the eighth nerve. Stypulkowski and van den Honert (1984) propose two mechanisms to explain this phenomenon with respect to their *N1* recovery functions (p. 220), both of which depend on the existence of intact dendrites. However, it is not clear whether the mechanisms they propose are consistent with the Miller *et al.* data (1993), in which nonmonotonicities at 1–2 ms were observed for both wave Ia (presumed axonal) and wave Ib (presumed dendritic) responses.

A second possible explanation for facilitation in the present data involves loudness summation. White *et al.* (1984) observed in one subject that the loudness of two equal-amplitude pulses increased considerably as inter-pulse separation was reduced from 6 ms to 0.5 ms. This implies that significant loudness summation can occur when two pulses are presented in close succession. Consistent with this, our subjects frequently reported using a loudness cue to discriminate the signal interval at short time delays (1–2 ms), but reported different perceptual cues (e.g., hearing two separate pulses) at longer time delays. Because loudness summation decreases with interpulse interval, this explanation is consistent with our observation that facilitation was greatest at the shortest time delays.

Loudness summation can also account for the fact that facilitation tended to be larger at lower masker levels than at higher masker levels. At the short time delays where facilitation is observed, refractoriness prevents individual nerve fibers from responding to both the masker and probe pulses; thus, loudness summation can only occur when different groups of fibers respond to the two stimuli. High-level maskers elicit responses from a large proportion of stimulated fibers, leaving few fibers to respond to the probe. In contrast, low-level maskers excite a smaller proportion of fibers, with the result that many fibers are available to respond to the probe. Presuming that loudness summation increases with the number of fibers responding to the probe, then greater loudness summation should occur at low masker levels, as seen in the present data. A similar relationship between probability of response and loudness summation was recently proposed by McKay and McDermott (1998).

A related phenomenon has been observed in single-unit neural responses to subthreshold pulse pairs (Eddington *et al.*, 1978; Butikofer and Lawrence, 1979; Dynes and Delgutte, 1995; Eddington *et al.*, 1995). When subthreshold pulses are presented in pairs, with a short time delay between them (<4 ms), they can elicit a neural response even though the pulses are up to 6 dB below their individual neural excitation thresholds. Whether the physiological mechanisms underlying the present demonstrations of suprathreshold facilitation are the same as those responsible for such subthreshold facilitation is not known. However, it is interesting that the largest suprathreshold facilitation is seen at lower masker levels. Additional studies are needed to quantify the facilitation effects observed here in SPFM, to determine whether they are related to subthreshold facilitation, and to determine how such facilitation effects might modify the perceptions of longer pulse trains.

### I. Correlations with word recognition

A significant negative correlation was obtained in this study between SPFM recovery time constants for basal electrodes and word recognition scores. This finding echoes results previously reported for EAP measures of refractoriness (Brown *et al.*, 1990), but is primarily due to the data for two subjects (AGF and EJQ) who demonstrated the lowest speech scores. In addition, it is not clear why correlation coefficients were not significant for middle and apical electrodes. Evaluation of similar measures in a much larger population of cochlear implant listeners is needed to clarify possible relationships between SPFM time constants and performance on speech recognition tests.

### V. CONCLUSIONS

Recovery from single-pulse psychophysical forward masking can be described by an exponential recovery process in which the amount of threshold shift (in  $\mu\text{A}$ ) produced by a single-pulse masker recovers exponentially in time. Time constants average 5.5 ms across subjects and electrodes, with a standard error of 0.75 ms. Time constants are independent of masker level and do not vary systematically

with electrode location. However, they can differ significantly with electrode location in individual subjects.

Response to the masker grows linearly with masker level (in  $\mu\text{A}$ ) at a time delay of 0 ms. Growth rates at longer time delays are shallower than 1, and are determined by the level-independent time constant. This behavior is consistent with an exponential recovery process.

The addition of a constant residual threshold shift improves the exponential fit to most SPFM recovery curves, consistent with the existence of a second, slower recovery process. In some cases, the slower recovery process is sufficiently well defined to be fitted with a second exponential process with a longer time constant.

The rapid-recovery process of psychophysical SPFM has a time constant less than 5–7 ms, consistent with eighth-nerve refractoriness. The slower recovery process exhibits time constants that are too long to attribute to eighth-nerve refractoriness and likely reflects more central processes.

Prolonged time constants for the rapid-recovery process (>7 ms) may reflect altered mechanisms of neural excitation associated with long-term deafness.

There is some evidence that prolonged SPFM time constants are associated with poor speech recognition; however, a larger data set is needed to better evaluate this possibility.

### ACKNOWLEDGMENTS

This work was supported by NIDCD grant DC00110 and by the Lions 5M International Hearing Foundation. John Van Essen converted Robert Shannon's computer software into the C language and made modifications to that software for carrying out the present research. Tanya Grann, Shanna Allen, Tara Khetrepal, and Ying-Yee Kong assisted with data collection, and Magda Wojtczak provided helpful comments on an earlier version of the paper. Cochlear Corporation provided subjects' calibration tables. The authors would like to extend special thanks to the eight subjects who participated in this work.

<sup>1</sup>Facial nerve stimulation restricted electrode selection in two subjects (AGF and DAW). For these subjects, test electrodes were distributed across the range of stimulable electrodes.

<sup>2</sup>The ordinate in Fig. 1 is shown in linear units ( $\mu\text{Amps}$ ) of threshold shift to illustrate that masked threshold recovers asymptotically to absolute probe threshold, i.e., the recovery process involves the recovery of an *effect* (threshold shift) to zero, not the recovery of a physical stimulus down to some physical reference. All later figures express masked thresholds in this way (i.e., they show threshold shift in  $\mu\text{Amps}$  on the ordinate). The abscissa in Fig. 1 is shown in linear units of time delay between masker and probe to illustrate the exponential nature of the recovery process. Because the range of time delays evaluated in this experiment is large, later figures use a logarithmic scale to show time delay on the abscissa.

<sup>3</sup>A CSU is the smallest change in current realizable with the implanted stimulator. The decibel step size corresponding to one CSU varies slightly across the dynamic range and among individual implanted stimulators, but is usually between 0.1 and 0.3 dB.

<sup>4</sup>Fittable SPFM recovery curves at two or more masker levels were obtained from only seven of the subjects, because AMB's recovery curves were only well fit for the highest masker level. Of those seven subjects, one electrode exhibited a negative slope (AGFr12), which was not included in the averages across electrodes reported here.

Abbas, P. J., and Brown, C. J. (1991). "Electrically evoked auditory brainstem response: Refractory properties and strength-duration functions," *Hear. Res.* **51**, 139–148.

- Abbas, P. J., and Gorga, M. P. (1981). "AP responses in forward-masking paradigms and their relationship to responses of auditory-nerve fibers," *J. Acoust. Soc. Am.* **69**, 492–499.
- Blamey, P. J., and Dooley, G. J. (1993). "Pattern recognition and masking in cochlear implant patients," in *Progress in Brain Research*, edited by J. H. J. Allison, D. J. Allison-Mecklenburg, F. P. Harris, and R. Probst (Elsevier Science, New York), Vol. 97, pp. 271–278.
- Brown, C. J., Abbas, P. J., Borland, J., and Bertschy, M. R. (1996). "Electrically evoked whole nerve action potentials in Ineraid cochlear implant users: Responses to different stimulating electrode configurations and comparison to psychophysical responses," *J. Speech Hear. Res.* **39**, 453–467.
- Brown, C. J., Abbas, P. J., and Gantz, B. J. (1990). "Electrically evoked whole-nerve action potentials: Data from human cochlear implant users," *J. Acoust. Soc. Am.* **88**, 1385–1391.
- Brown, C. J., Abbas, P. J., Hughes, M. L., Parkinson, A., and Tyler, R. (1999). "Relationship between EAP growth and recovery functions measured using the Nucleus neural response telemetry software and psychophysical measures of loudness and speech perception," presented at the Conference on implantable auditory prostheses, Asilomar Conference Center, Pacific Grove, California.
- Buttkofer, R., and Lawrence, P. D. (1979). "Electrocutaneous nerve stimulation: II. Stimulus waveform selection," *Izv. Akad. Nauk SSSR, Ser. Geogr. Geofiz.* **26**, 69–75.
- Donaldson, G. S., and Nelson, D. A. (1999). "Single-pulse and pulse-train forward masking functions: Do they reflect different neural recovery processes," presented at the 1997 Conference on Implantable Auditory Prostheses, Pacific Grove, California.
- Duifhuis, H. (1973). "Consequences of peripheral frequency selectivity for nonsimultaneous masking," *J. Acoust. Soc. Am.* **54**, 1471–1488.
- Dynes, S., and Delgutte, B. (1995). "Temporal interactions of electric pulses in the auditory nerve: experiments and modeling," presented at the Proceedings of the 1995 Conference on Implantable Auditory Prostheses, Pacific Grove, California.
- Eddington, D. K., Doebelle, W. H., Brackmann, D. E., Mladejovsky, M. G., and Parkin, J. L. (1978). "Auditory prostheses research with multiple channel intracochlear stimulation in man," *Ann. Otol. Rhinol. Laryngol.* **87**, 5–39.
- Eddington, D. K., Long, C. J., Rubinstein, J. T., and Whearty, M. E. (1995). "Minimizing nonsimultaneous interactions," presented at the Proceedings of the 1995 Conference on Implantable Auditory Prostheses, Pacific Grove, California.
- Hong, S. H., Brown, C. J., Hughes, M. L., and Abbas, P. J. (1998). "Electrically evoked compound action potentials using neural response telemetry in CI24M: Refractory recovery function of the auditory nerve," ARO Abstracts, #288.
- Hong, S. H., Hughes, M. L., Abbas, P. J., Brown, C. J., Gervais, J. P., Wolaver, A. A., and Gantz, B. J. (1998). "Temporal response measures of the electrically evoked compound action potential (EAP) using the neural response telemetry system of the Nucleus CI24M device," presented at the 7th Symposium on Cochlear Implants in Children, Iowa City.
- Leake, P. A., and Hradek, G. T. (1988). "Cochlear pathology of long term neomycin induced deafness in cats," *Hear. Res.* **33**, 11–34.
- Levitt, H. (1971). "Transformed up-down methods in psychoacoustics," *J. Acoust. Soc. Am.* **49**, 467–477.
- Markman, N. D. (1989). "Recovery from forward masking in listeners with normal hearing, sensorineural hearing loss, and simulated hearing loss," Masters thesis, University of Minnesota.
- McKay, C. M., and McDermott, H. J. (1998). "Loudness perception with pulsatile electrical stimulation: The effect of interpulse intervals," *J. Acoust. Soc. Am.* **104**, 1061–1074.
- Miller, C. A., Abbas, P. J., and Robinson, B. K. (1993). "Characterization of wave I of the electrically evoked auditory brainstem response in the guinea pig," *Hear. Res.* **69**, 35–44.
- Nelson, D. A., and Freyman, R. L. (1987). "Temporal resolution in sensorineural hearing-impaired listeners," *J. Acoust. Soc. Am.* **81**, 709–720.
- Nelson, D. A., and Pavlov, R. (1989). "Auditory time constants for off-frequency forward masking in normal-hearing and hearing-impaired listeners," *J. Speech Hear. Res.* **32**, 298–306.
- Oxenham, A. J., and Moore, B. C. J. (1995). "Additivity of masking in normally hearing and hearing-impaired subjects," *J. Acoust. Soc. Am.* **98**, 1921–1934.
- Paintal, A. S. (1966). "The influence of diameter of medulated nerve fibers of cat on the rising and falling phases of the spike and its recovery," *J. Physiol. (London)* **184**, 791–811.
- Schuknecht, H. F. (1974). *Pathology of the Ear* (Harvard University Press).
- Shannon, R. V., Adams, D. D., Ferrel, R. L., Palumbo, R. L., and Grandgenett, M. (1990). "A computer interface for psychophysical and speech research with the Nucleus cochlear implant," *J. Acoust. Soc. Am.* **87**, 905–907.
- Stypulkowski, P. H., and van den Honert, C. (1984). "Physiological properties of the electrically stimulated auditory nerve. I. Compound action potential recordings," *Hear. Res.* **14**, 205–223.
- White, R. L., Merzenich, M. M., and Gardi, J. N. (1984). "Multichannel cochlear implants. Channel interactions and processor design," *Arch. Otolaryngol.* **110**, 493–501.
- Zeng, F. G., and Shannon, R. V. (1992). "Loudness balance between electric and acoustic stimulation," *Hear. Res.* **60**, 231–235.
- Zhou, R., Abbas, P. J., and Assouline, J. G. (1995). "Electrically evoked auditory brainstem response in peripherally myelin-deficient mice," *Hear. Res.* **88**, 98–106.